

Two dimensionally patterned $\text{GaN}_x\text{As}_{1-x}/\text{GaAs}$ nanostructures using N^+ implantation followed by pulsed laser melting

Taeseok Kim,^{a)} Michael J. Aziz, and Venkatesh Narayanamurti
Harvard School of Engineering and Applied Sciences, Cambridge, Massachusetts 02138, USA

(Received 16 July 2008; accepted 26 August 2008; published online 12 September 2008)

We present measurements on two dimensionally patterned $\text{GaN}_x\text{As}_{1-x}$ dots fabricated in a GaAs matrix using ion implantation followed by pulsed laser melting and rapid thermal annealing. The lithographically patterned $\text{GaN}_x\text{As}_{1-x}$ regions are imaged by ballistic electron emission microscopy (BEEM). By analyzing the BEEM spectra of the locally confined dots, we observe the decrease in the Schottky barrier height with nitrogen incorporation. The second derivatives of BEEM currents from unpatterned $\text{GaN}_x\text{As}_{1-x}$ films exhibit a decrease in Γ -like thresholds as the nitrogen concentration increases. The composition dependence of the thresholds agrees well with that of previously studied low temperature molecular beam epitaxy grown alloys. © 2008 American Institute of Physics. [DOI: 10.1063/1.2982424]

Highly mismatched semiconductor alloys (HMAs) have become important due to their dramatic changes in electronic properties from the host materials and motivated many potential technological applications.¹ $\text{GaN}_x\text{As}_{1-x}$ is a HMA known especially for its large bandgap reduction of as much as 180 meV per $x=0.01$ up to a few percent.^{2,3} Although thin films of this material have been well studied, for two dimensionally (2D) patterned devices, the composition must be controlled not only in the growth direction but also in the lateral directions. The synthesis of quantum dots and quantum wires has been largely based on spontaneous growth processes using the lattice mismatch and wetting behavior between substrates and the depositing materials.^{4,5} Ion implantation (II) followed by a combination of pulsed laser melting (PLM) and rapid thermal annealing (RTA) has recently been shown to produce high quality thin films of $\text{GaN}_x\text{As}_{1-x}$.^{6,7} The extremely fast (<100 ns) melting and solidification rates in the PLM process result in highly supersaturated substitutional solid solutions⁸ giving rise to a large bandgap reduction comparable to that in alloys grown by conventional thin film growth methods. Hence patterning the II followed by unpatterned transient thermal processing might permit the 2D patterning of the conduction band edge, thereby enabling the development of a variety of 2D quantum devices from HMAs.

Ballistic electron emission microscopy (BEEM) is a three-terminal scanning tunneling microscope (STM) that has been used to measure the electronic band structure of a buried semiconductor heterostructure by collecting carriers filtered by the Schottky barrier at the metal-semiconductor interface.⁹ Using BEEM, self-assembled quantum dots embedded in III-V semiconductors have been imaged and the resonant behaviors observed with nanometer scale spatial resolution.^{10,11} BEEM measurements on $\text{GaN}_x\text{As}_{1-x}$ thin films grown by low temperature molecular beam epitaxy (LT-MBE) have shown a decreasing Schottky barrier height with increasing nitrogen concentration.¹² In this letter, we use BEEM and spectrometry to characterize 2D patterned $\text{GaN}_x\text{As}_{1-x}$ nanostructures fabricated using patterned nitro-

gen implantation followed by PLM and RTA.

A 200 nm undoped GaAs layer was grown on a (001)-oriented n^+ GaAs substrate. For 2D patterning, a polymethyl methacrylate (PMMA) mask created by electron-beam lithography was used. The 400 nm thick mask has an array of holes of 75 nm diameter and 1.2 μm of period over a $600 \times 600 \mu\text{m}^2$ area. Nitrogen ions (N^+) were implanted onto the mask, which is designed to be thick enough to block all the implanted ions except those traversing the holes. By using an ion energy of 20 keV with different doses from 0.9×10^{15} to $4.6 \times 10^{15}/\text{cm}^2$, the selectively exposed GaAs regions were implanted down to ~ 100 nm depth with N atomic concentration from 1.3×10^{20} to $6.8 \times 10^{20}/\text{cm}^3$ at the peak of the distribution. For comparison, some samples were implanted without the mask under identical implantation conditions and will be referred to as planar-processed samples.

After lifting off the PMMA mask with the help of oxygen plasma ashing,¹³ the GaAs samples were pulsed laser melted in air using a XeCl excimer laser ($\lambda=308$ nm) with a pulse duration of ~ 30 ns full width at half maximum. Through a multiprism beam homogenizer, the laser formed a uniform rectangular shape spot with less than 4% rms intensity variation. The melt durations (τ_{melt}) were determined by measuring the time resolved reflectivity of the samples using a low-power continuous-wave argon-ion (488 nm) probe laser. The excimer laser fluence at the sample ranged between 0.27 and 0.33 J/cm^2 , corresponding to 55 and 99 ns of melt duration from the planar-processed samples. Some of the samples were treated by RTA after PLM at temperatures between 850 and 950 °C for 5 to 10 s in flowing N_2 , as reported in a previous study.⁶

To make samples for BEEM, Cr/Au Ohmic contacts were deposited to the bottom of the n^+ GaAs substrates, and for Schottky contacts, Au layers (8 nm thick) were deposited on the samples by thermal evaporation at a typical background pressure of 3×10^{-7} torr. Prior to Au evaporation, the pulsed laser melted GaAs surfaces were treated in a 1:10 solution of $\text{NH}_4\text{OH}:\text{H}_2\text{O}$ for 60 s followed by ~ 3 s rinse in de-ionized water. The Au contacts were 0.9 mm in diameter and made by photolithography.¹⁴ The BEEM measurements were performed in air at room temperature with a surface/

^{a)}Electronic mail: kim57@fas.harvard.edu.

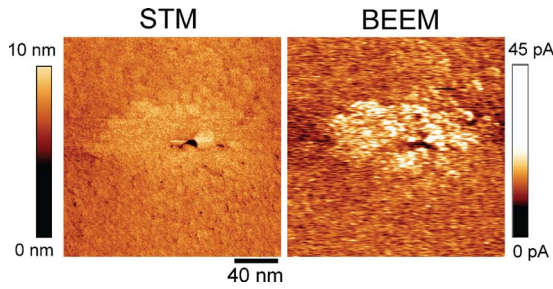


FIG. 1. (Color online) STM and BEEM images of one of the implanted $\text{GaN}_x\text{As}_{1-x}$ dots. Both images are measured simultaneously at $V_T = -1.0$ V and $I_T = 2$ nA. The Au grains and N^+ -implanted dot (~ 120 nm diameter in the center) are visible in the STM image, and an enhancement in the BEEM current is observed at the implanted region. The sample was implanted with $1.77 \times 10^{15}/\text{cm}^2$ of N^+ at 20 keV, followed by 0.31 J/ cm^2 of PLM and RTA at 950°C for 10 s.

interface AIVTB-4 BEEM/STM system using a Au tip.

Figure 1 shows the STM and BEEM image of a dot made by patterned implantation followed by PLM and RTA. In the STM image, the Au grains (~ 10 nm) and the N^+ -implanted region are visible. The original implanted dot diameter of 80 nm has been enlarged to about 120 nm, which is likely due to the lateral diffusion of nitrogen during PLM. The BEEM image was taken simultaneously while the tunneling current (I_T) was set to 2 nA and the tip voltage (V_T) is fixed at -1.0 V, which is above the Schottky barrier height for the Au/GaAs interface. A strong enhancement (~ 5 pA) in the BEEM current is observed within the patterned region implanted with $1.77 \times 10^{15}/\text{cm}^2$ of N^+ at 20 keV, corresponding to $x \sim 0.005$ estimated from the secondary ion mass spectrometry (SIMS) on the planar-processed samples.

To confirm the source of this higher BEEM current on the dot region, BEEM spectra were taken on and off the dot. Figure 2 shows the BEEM spectra averaged over 200 voltage scans for each region in order to increase the signal to noise ratio. The thresholds were inferred from a two valley Bell-Kaiser (B-K) model least-squares fit using

$$I_c(V) = R_{\Gamma,L} I_T \frac{\int_{E_{z,\min}}^{\infty} D(E_z, V) \int_0^{E_{t,\max}} F(E) dE_t dE_z}{\int_0^{\infty} D(E_z, V) \int_0^{\infty} [F(E) - F(E+eV)] dE_t dE_z},$$

where V is the tip bias, I_T is the tunneling current, D is the Wentzel-Kramer-Brillouin tunneling probability, and F is

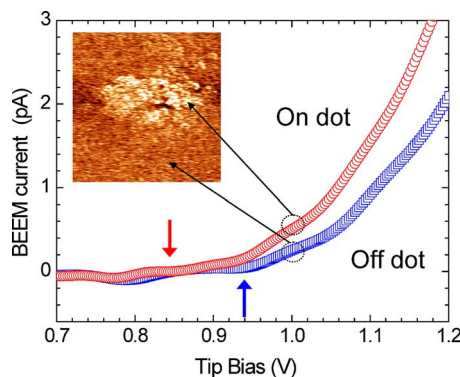


FIG. 2. (Color online) BEEM Spectra on and off the synthesized dot, exhibiting shift in thresholds on the dot at tip bias below the Schottky barrier height of unimplanted surrounding GaAs. The arrows indicate fitted thresholds for on dot (0.84 V) and off dot (0.93 V).

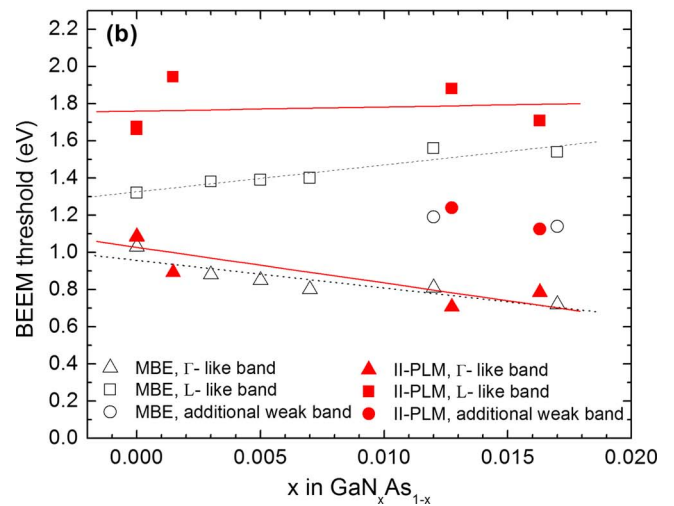
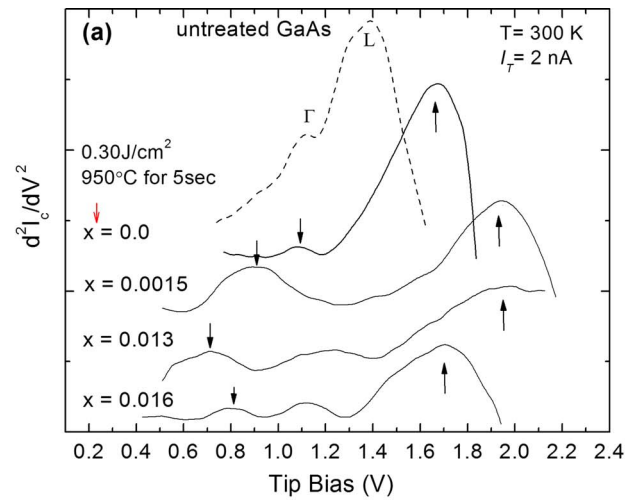


FIG. 3. (Color online) (a) SD-BEEM spectra for different nitrogen concentrations. The dotted line on top represents the SD spectra of unprocessed GaAs substrate without implantation. (b) Compositional dependence of thresholds observed at the peaks of the SD-BEEM spectra of $\text{GaN}_x\text{As}_{1-x}$. The open symbols are the thresholds for LT-MBE grown $\text{GaN}_x\text{As}_{1-x}$ (Ref. 12) and the solid symbols are for the thresholds for II-PLM-RTA $\text{GaN}_x\text{As}_{1-x}$ measured in this paper. The lines are linear fits of the concentration dependency for MBE grown (dotted) and II-PLM (solid) samples.

the Fermi function. The integration limits are determined by transverse momentum conservation and set to $E_{z,\min} = E_F - e(V - V_{b\Gamma,bL})$ and $E_{t,\max} = m_t/(m - m_t)[E_z - E_F + e(V - V_{b\Gamma,bL})]$. E_F is the Fermi energy in the Au tip and $m_t(m)$ is the transverse effective mass in the semiconductor (metal). $R_{\Gamma,L}$ and $V_{b\Gamma,bL}$ are the attenuating factors and the Schottky barriers related to the Γ or L valley transition, respectively, and used as adjustable parameters during fitting.^{14,15} The fitting results exhibit a shift in the initial Γ threshold from 0.93 to 0.84 V when the tip moves from the surrounding GaAs to the patterned dot area, as indicated by the arrows. The small structures in the off-dot spectra below the main threshold of 0.93 V represent fluctuation in the signal to noise. Significant BEEM current is measurable only above about 0.9 V for the off-dot spectra, and we used the data as a starting point for the B-K fitting. The kink at around 0.9 V of the on-dot spectra might be real and related to the buried undoped GaAs left between the nitrogen implanted depth (~ 100 nm) and the n^+ GaAs substrate. The nitrogen implanted sample, however, shows measurable BEEM current at lower threshold

Schottky barrier, and the simple B–K fitting was intended to simply get the lowest thresholds in this study. This threshold reduction, which is at least four times the room temperature thermal energy of electrons, opens the possibilities of producing an arbitrarily patterned quantum confined structure using II and PLM, and of imaging the structure with BEEM.

To investigate the nitrogen concentration dependence of the threshold [Fig. 3(a)], we compare the second derivative (SD) BEEM spectra of the planar-processed $\text{GaN}_x\text{As}_{1-x}$ implanted without a mask at 20 keV and four different doses, followed by 0.30 J/cm^2 of PLM and RTA at 950°C for 5 s. The nitrogen concentrations after PLM and RTA were determined by averaging over the maximum laser melting depths the nitrogen concentration-depth profile as determined by SIMS. The room temperature SD-BEEM spectra extracted from the experimental BEEM spectra are approximately the heterostructure transmission coefficients of the collector current, so that features in the spectra can be used to identify specific hot electron transport channels.¹⁶ The dotted line on top represents the SD spectra of an unprocessed GaAs substrate without implantation, laser melting, or RTA; the two main peaks can be identified as the Γ and L peaks of GaAs as in the previous study.¹² It is apparently shown that the peaks for the II-PLM samples located by arrows are shifted from the corresponding peaks for the unprocessed GaAs. In Fig. 3(b), we compare the energies of those peaks (thresholds) of II-PLM samples with corresponding measurements for LT-MBE grown $\text{GaN}_x\text{As}_{1-x}$ (Ref. 12) as a function of the nitrogen concentration. The lines are linear fits for the concentration dependence of the thresholds in MBE grown (dotted) and II-PLM (solid) samples. The Γ -like thresholds (Schottky barriers for $\text{Au}/\text{GaN}_x\text{As}_{1-x}$) decrease as the nitrogen concentration increases for both fabrication routes. The linear fit to the Γ -like peaks for the II-PLM samples gives a slope of $-19.1 \pm 6.3 \text{ eV}$, which is comparable to the corresponding slope (-16.4 eV) for the LT-MBE grown samples. The deviation from the linear fit for Γ -like thresholds of II-PLM samples may be due to the increased surface scattering for the laser melted samples.

In conclusion, we have shown 2D patterned $\text{GaN}_x\text{As}_{1-x}$ nanostructures fabricated using II-PLM and RTA and imaged using BEEM. The analysis of the BEEM current on the locally confined $\text{GaN}_x\text{As}_{1-x}$ dots exhibits a strong decrease in the $\text{Au}/\text{GaN}_x\text{As}_{1-x}$ Schottky barrier with nitrogen incorporation. The SD-BEEM spectra from unpatterned $\text{GaN}_x\text{As}_{1-x}$ ($x=0.0-0.016$) show two main peaks, which can be attrib-

uted to contributions from Γ - and L -like bands. We found a decrease in Γ -like thresholds as the nitrogen concentration increases. The composition dependency of the first Γ -like thresholds is comparable to the previously studied LT-MBE grown alloys.

We thank Kirstin Alberi and Oscar Dubon for technical assistance and valuable discussions. This work was supported by a Defense Advanced Research Projects Agency HUNT (Grant No. 222891-01) subaward from the University of Illinois at Urbana-Champaign and by the National Science Foundation under Grant No. NSF-ECCS-0701417. The support of the Center for Nanoscale Systems (CNS) at Harvard University is also acknowledged. Harvard-CNS is a member of the National Nanotechnology Infrastructure Network (NNIN), which is supported by the National Science Foundation under Grant No. ECS-0335765. RTA of samples was supported by the Director, Office of Science, Office of Basic Energy Sciences, Division of Materials Sciences and Engineering, of the (U.S.) Department of Energy under Grant No. DE-AC02-05CH11231.

¹J. W. Ager and W. Walukiewicz, *Semicond. Sci. Technol.* **17**, 741 (2002).

²K. Uesugi, N. Morooka, and I. Suemune, *Appl. Phys. Lett.* **74**, 1254 (1999).

³M. Kondow, K. Uomi, K. Hosomi, and T. Mozume, *Jpn. J. Appl. Phys., Part 2* **33**, L1056 (1994).

⁴P. M. Petroff, A. Lorke, and A. Imamoglu, *Phys. Today* **54**(5), 46 (2001).

⁵Q. Xie, A. Madhukar, P. Chen, and N. P. Kobayashi, *Phys. Rev. Lett.* **75**, 2542 (1995).

⁶K. M. Yu, W. Walukiewicz, J. W. Beeman, M. A. Scarpulla, O. D. Dubon, M. R. Pillai, and M. J. Aziz, *Appl. Phys. Lett.* **80**, 3958 (2002).

⁷K. M. Yu, W. Walukiewicz, M. A. Scarpulla, O. D. Dubon, J. Wu, J. Jasinski, Z. Liliental-Weber, J. W. Beeman, M. R. Pillai, and M. J. Aziz, *J. Appl. Phys.* **94**, 1043 (2003).

⁸M. J. Aziz, *Metall. Mater. Trans. A* **27**, 671 (1996).

⁹V. Narayanamurti and M. Kozhevnikov, *Phys. Rep.* **349**, 447 (2001).

¹⁰M. E. Rubin, G. Medeiros-Ribeiro, J. J. O'Shea, M. A. Chin, E. Y. Lee, P. M. Petroff, and V. Narayanamurti, *Phys. Rev. Lett.* **77**, 5268 (1996).

¹¹M. E. Rubin, H. R. Blank, M. A. Chin, H. Kroemer, and V. Narayanamurti, *Appl. Phys. Lett.* **70**, 1590 (1997).

¹²M. Kozhevnikov, V. Narayanamurti, C. V. Reddy, H. P. Xin, C. W. Tu, A. Mascarenhas, and Y. Zhang, *Phys. Rev. B* **61**, R7861 (2000).

¹³J. I. McOmber, K. Ostrowski, M. Meloni, R. Eddy, and P. Buccos, *Nucl. Instrum. Methods Phys. Res. B* **74**, 266 (1993).

¹⁴J. J. O'Shea, E. G. Brazel, M. E. Rubin, S. Bhargava, M. A. Chin, and V. Narayanamurti, *Phys. Rev. B* **56**, 2026 (1997).

¹⁵L. D. Bell and W. J. Kaiser, *Phys. Rev. Lett.* **61**, 2368 (1988).

¹⁶D. L. Smith and S. M. Kogan, *Phys. Rev. B* **54**, 10354 (1996).